

# A SYSTEMATIC METHODOLOGY FOR OPTIMAL COMPONENT SELECTION OF ELECTROHYDRAULIC SERVO SYSTEMS

Evangelos Papadopoulos and Ioannis Davliakos

*Dept. of Mechanical Engineering, National Technical University of Athens, 15780 Athens, Greece  
egpapado@central.ntua.gr, gdavliak@central.ntua.gr*

---

## Abstract

This paper focuses on optimal hydraulic component selection for electrohydraulic systems used in high performance servo tasks. Dynamic models of low complexity are proposed that describe the salient dynamics of basic electrohydraulic equipment. Rigid body equations of motion, the hydraulic dynamics and typical trajectory inputs are used in conjunction with optimization techniques, to yield an optimal hydraulic servosystem design with respect to a number of criteria such as cost, weight or power. The optimization procedure employs component databases with real industrial data, resulting in realizable designs. An example illustrates the developed methodology.

**Keywords:** electrohydraulic servosystem, optimization, optimal design

---

## 1 Introduction

Recently, the combination of the hydraulics science with servo control, also called hydrotronics, has given new thrust to hydraulics applications (Six and Lasky, 2001). The main reasons why hydrotronics are preferred in some applications to electromechanical drives include their ability to produce large forces at high speeds, their high durability and stiffness, and their rapid response (Jelali and Kroll, 2003). Hydraulic control components and servosystems are found in many mobile, airborne and stationary applications (Moog, Parker).

However, hydraulic systems are inherently nonlinear and their operation differs significantly from that of electromechanical drives. Due to a lack of substantial formal training in hydraulic technology, engineers and practitioners select components and design such systems based either on experience and past successful designs, or with the help of simplified manufacturer design examples. In both cases, designs tend to depend on a single operating point, or a simple cycle. However, most high performance servo tasks, robotic tasks included, contain complex, time-varying trajectories which cannot be handled easily. For example, the apparent mass and gravity load that is seen by a hydraulic actuator of a six degrees-of-freedom (dof) Stewart platform (Stewart, 1965-66) changes dramatically according to the commands

given. Therefore, it is normal that designs based on experience or isolated operating points tend to be oversized, resulting in overall inefficient servos.

Early work on hydraulic systems optimization has been presented (Krus and Jansson, 1991) that introduces a set of performance parameters uniquely defining system components. This approach requires extensive component modelling aiming at the identification of the appropriate set of performance parameters. A design procedure for actuator control systems that is based on a few mechanical specifications (Hansen and Andersen, 2001) using optimization methods has been studied. This method is based on reducing energy consumption, taking into consideration stability, load independency, response and manufacturability criteria. The design and dynamic behaviour of a hydraulically actuated loader crane has been presented (Hansen et al, 2001). A minimization problem is formulated with a view to optimize an existing commercial available hydraulic loader crane, bound by life, weight, controllability and efficiency criteria. An important application of dynamic modeling is component sizing. A method for sizing proportional servovalves of a forestry machine with a given hydraulic supply has been proposed (Papadopoulos and Sarkar, 1997). A non-systematic sizing of a hydraulic servo for robotic tasks that used dynamic modeling has been discussed, see (Chatzakos and Papadopoulos, 2003; Chatzakos, 2002).

For electromechanical systems, optimal servo-mechanism design has been studied recently. The optimal electric motor selection for robots has been studied (Bowling and Khatib, 2002). Related research, based on the technical features of electric servomotors, has been presented, see (Van de Straete et al, 1998).

This paper focuses on the optimal electrohydraulic component selection for servohydraulic robotic tasks. The proposed methodology requires as its input a set of desired trajectories of the controlled mechanism and a description of the mechanism itself. Outputs include the complete specification of the system components such as the electric motor, the hydraulic pump, the hydraulic accumulator, the servovalve and the hydraulic servoactuator. Dynamic models for the electrohydraulic actuation system and its mechanical load (mechanism) are used to compute the best design parameters that minimize an objective function that may include the hydraulic supply power rating, the total weight, or the total cost. To this end, the Sequential Quadratic Programming (SQP) is employed as the optimization algorithm (Biggs, 1975; Han, 1977). The optimization procedure uses component databases with real industrial data, resulting in realizable designs. The paper presents a detailed example in which the proposed methodology is applied.

## 2 Structure of Electrohydraulic Servosystems

In this section, the structure of electrohydraulic servosystems actuating high performance mechanisms is presented briefly. An electrohydraulic servosystem consists of a servomechanism, including a servovalve, a servoactuator, a controller, a mechanical load and a hydraulic power supply. The controller can be realized on a PC with control cards, or by standalone servoamplifiers. Power supplies include an electric motor, a hydraulic pump, pressure regulators, hydraulic accumulators, hydraulic tanks, oil coolers, safety, relief and auxiliary valves, hydraulic filters and hoses. Next, simple models of major components are described.

### 2.1 Dimensioning of Servomechanism

Primary parameters in servomechanism design include specifications such as hydraulic motor volumetric displacement, piston areas, system pressure and flow, servovalve flow, etc.

During the design stage of a hydraulic servo, oil compressibility and leakages in hoses, filters, relief and auxiliary valves, can be neglected (Papadopoulos and Gonthier, 2002). An ideal hydraulic motor is described by the following transduction equations

$$Q_{L,m} = D_m \dot{\theta}_m \quad (1a)$$

$$\Delta p_{L,m} = p_{L,m1} - p_{L,m2} = D_m^{-1} T_m \quad (1b)$$

where  $Q_{L,m}$  is the flow through the motor,  $D_m$  is its radian displacement,  $\theta_m$  is its angular position,  $\Delta p_{L,m}$  is the pressure drop across the motor,  $p_{L,m1}$  is the pressure in the forward chamber of the motor,  $p_{L,m2}$  is the pressure in its return chamber and  $T_m$  is the motor output torque. A real hydraulic motor includes leakage flows and friction. Using continuity equations, the load flow is given by

$$Q_{L,m} = D_m \dot{\theta}_m + (C_{im} + C_{em}/2) \Delta p_{L,m} \quad (2)$$

where  $C_{im}$  is the internal or cross-port leakage coefficient and  $C_{em}$  is the external leakage coefficient (Merritt, 1967).

An ideal single rod hydraulic cylinder is described by

$$Q_{L,p1} = A_1 \dot{x}_p \quad (3a)$$

$$Q_{L,p2} = A_2 \dot{x}_p \quad (3b)$$

$$p_{L,p1} A_1 - p_{L,p2} A_2 = F_p \quad (3c)$$

where  $Q_{L,p1}$ ,  $Q_{L,p2}$  are the flows through its two chamber ports,  $p_{L,p1}$ ,  $p_{L,p2}$  are the chamber pressures,  $A_1$  is the piston side area,  $A_2$  is the rod side area,  $x_p$  is the piston displacement and  $F_p$  is the piston output force. A real cylinder model also includes chamber oil compressibility, friction and other effects. However, these can be neglected at an initial stage.

Control of hydraulic systems is achieved through the use of servovalves. Only the resistive effect of a valve is considered here, since their natural frequency is much higher than that of the hydraulics and mechanical load. It is also assumed that the geometry of the valve is ideal, e.g. sharp edges, zero cross leakages (Blackburn et al, 1960; Thayer, 1962). The valve elemental (orifice) equations for the two symmetrical orifices is

$$\Delta p_{v,i} = C_R Q_{v,i} |Q_{v,i}|, \quad i = 1, 2 \quad (4)$$

where  $\Delta p_{v,i}$  is the valve pressure drop at each valve orifice,  $Q_{v,i}$  is the corresponding flow through an orifice and  $C_R$  is a coefficient, which depends on the orifice area  $S$ , the discharge coefficient  $C_d$  and the mass density of the fluid  $\rho$ ,

$$C_R = 0.5 \rho C_d^{-2} S^{-2} \quad (5)$$

In general, the discharge coefficient is as function of the *Reynolds* number and valve geometry, when the short tube orifice flow is turbulent. However, it can be approximated by a constant (Merritt, 1967).

In the case of an ideal hydraulic cylinder with a double rod, the two areas  $A_1$  and  $A_2$  are equal and therefore, Eq. 3 become:

$$Q_{L,p} = A \dot{x}_p \quad (6a)$$

$$\Delta p_{L,p} = F_p A^{-1} \quad (6b)$$

Where  $Q_{L,p}$  is the flow through the valve,  $\Delta p_{L,p}$  is the pressure drop across the cylinder and  $A$  is the piston active area. The valve elemental (orifice) equation, in this case, is given by

$$\Delta p_v = C_R Q_v |Q_v| \quad (7)$$

where  $\Delta p_v$  is the valve pressure drop across the valve and  $Q_v$  is the flow through it.

Eq. 4 or 7 can be used to plot valve flow versus valve drop for various orifice openings. For example, Fig. 1 displays the flow through a valve for an orifice open 30%, 60% and 100%. If the orifice area is open 100%, then the nominal flow through the valve,  $Q_{v,nom}$ , is usually the one that corresponds to a nominal pressure  $\Delta p_{v,nom} = 7$  MPa, see Fig. 1.

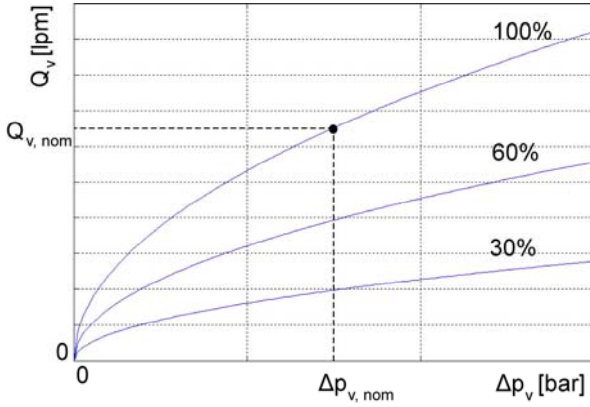


Fig. 1: A typical flow-pressure drop servovalve curve

## 2.2 Hydraulic Power Supply

Hydraulic power units regulate and supply the required hydraulic power of the servo plant. Hydraulic pumps are usually constant pressure piston pumps, which supply the servosystem with power, given by

$$P = p_s Q_s \quad (8)$$

where  $p_s$  is the pump output pressure and  $Q_s$  is the pump supplied flow. Usually, the largest amount of this hydraulic power is dissipated by the servovalves, and the rest of the hydraulic energy is consumed mainly by the mechanical load requirements and secondary by the hoses and auxiliary valves of the system. Neglecting secondary effects (Papadopoulos and Gonthier, 2002), a simple pressure compatibility equation yields

$$p_s = \Delta p_v + |\Delta p_L| \quad (9)$$

where  $\Delta p_L$  is the pressure drop across a hydraulic motor, or a cylinder, given by

$$\Delta p_L = p_{L,1} - p_{L,2} \quad (10a)$$

where  $p_{L,1}$  and  $p_{L,2}$  are the chamber pressures of the motor or cylinder. In Eq. 9  $\Delta p_v$  is the servovalve pressure drop given by

$$\Delta p_v = \Delta p_{v1} + \Delta p_{v2} \quad (10b)$$

where  $\Delta p_{v1}$  and  $\Delta p_{v2}$  are the pressure drops at the servovalve ports given by

$$\Delta p_{v1} = p_s - p_{L,p1} \quad (11a)$$

$$\Delta p_{v2} = p_{L,p2} \quad (11b)$$

The pump is usually driven by an induction electric motor. Hydraulic supplies may include accumulators for filtering pressure pulsations from the pump, but also for allowing the use of smaller rating pumps by providing additional flow when needed. The element equation for an accumulator is given by

$$Q_c = C_f \frac{dp_c}{dt} \quad (12)$$

where  $Q_c$  is the fluid flow,  $p_c$  is the accumulator pressure charge or discharge and  $C_f$  is the hydraulic capacitance of the accumulator.

Finally, the hydraulic power supply selection is completed by the selection of appropriate auxiliary elements, such as the type of filtration.

## 2.3 Mechanical Load Dynamics

Neglecting external disturbances and forces / torques due to friction acting on the system, the equation of motion of a servomechanism can be written in the form

$$\mathbf{M}(q)\ddot{q} + \mathbf{V}(q, \dot{q}) + \mathbf{G}(q) = \boldsymbol{\tau} \quad (13)$$

where  $\mathbf{q}$  is the  $n \times 1$  vector of generalized coordinates,  $\mathbf{M}(q)$  is the  $n \times n$  positive definite mass matrix, the  $n \times 1$  vector  $\mathbf{V}(q, \dot{q})$  represents torques arising from centrifugal and Coriolis forces, the  $n \times 1$  vector  $\mathbf{G}(q)$  represents torques due to gravity and  $\boldsymbol{\tau}$  is the  $n \times 1$  vector of actuator joint torques.

## 2.4 Integrated System Equations

Hydraulic actuation dynamics can be written using a systems approach, such as the Linear Graph, (Rowell, 1997; Papadopoulos and Gonthier, 2002; Papadopoulos et al, 2003), or Bond Graph, (Rosenberg and Karnopp, 1983; Herman et al, 1992), methods. This results in a set of nonlinear state space equations. To integrate these models to the mechanical load dynamics, one needs to provide expressions transforming pressure differences to torques / forces, Eq. 1b and 3b and angular/translational velocities to flows, Eq. 1a and 3a. In general, hydraulic and load

dynamics are described by nonlinear equations of the form

$$\dot{\mathbf{x}} = \mathbf{f}(\mathbf{x}, \mathbf{u}, \mathbf{d}) \quad (14a)$$

$$\mathbf{y} = \mathbf{h}(\mathbf{x}, \mathbf{u}, \mathbf{d}) \quad (14b)$$

where  $\mathbf{x}$  is a state column vector,  $\mathbf{u}$  is the input column vector,  $\mathbf{y}$  is the output column vector and  $\mathbf{d}$  is the vector of design parameters (e.g. pressures, geometry features, etc).

### 3 Optimization Analysis

In this section, a systematic methodology for the generalized selection of electrohydraulic servosystems components is developed. This is achieved using a programming code, which takes into account the servosystem dynamics and an optimization algorithm minimizing a task - related objective function. Three optimization criteria are considered; namely, the minimization of the required hydraulic supply power, of the total weight and of the total cost. For this purpose the following three objective functions are defined

$$\mathcal{F}_1 = P(\mathbf{d}), \quad \mathcal{F}_2 = C(\mathbf{d}), \quad \mathcal{F}_3 = W(\mathbf{d}) \quad (15)$$

where  $P$  is the hydraulic power, which is supplied by the hydraulic pump, given by Eq. 8,  $C$  is the total system cost and  $W$  is the total system weight. The three quantities are expressed as functions of the system design parameters. Usually, the total weight and cost of such systems are approximately linear functions of power.

The selection of an electrohydraulic servosystem is achieved by an optimization algorithm, which is based on knowledge of the kinematic and dynamic parameters of the load and of its desired trajectories. Appropriate constraints have the form

$$\mathbf{g}_j(\mathbf{d}) \leq \mathbf{0}, \quad j \in I_1 = \{1, 2, \dots, p_1\} \quad (16a)$$

$$\mathbf{g}_j(\mathbf{d}) = \mathbf{0}, \quad j \in I_2 = \{p_1 + 1, p_1 + 2, \dots, p_1 + p_2\} \quad (16b)$$

where vector functions  $\mathbf{g}_j(\mathbf{d})$  are constraints, that depend on the nature of the electrohydraulic

servosystem. Mathematically, they represent a mapping from  $\mathbb{R}^n$  to  $\mathbb{R}^m$ , where  $n$  is the dimension of the design vector  $\mathbf{d}$ ,  $m = p_1$ , for Eq. 16a and  $m = p_2$ , for Eq. 16b. The optimization problem is then described mathematically as

$$\min_{\mathbf{d} \in \mathbb{R}^n} \left\{ \mathcal{F}(\mathbf{d}): \mathbf{g}_j(\mathbf{d}) \leq \mathbf{0}, \quad j \in I_1, \quad \mathbf{g}_j(\mathbf{d}) = \mathbf{0}, \quad j \in I_2 \right\} \quad (17)$$

where  $\mathcal{F}(\mathbf{d})$  is the vector of objective functions, with dimension  $s$  ( $\mathbb{R}^n \rightarrow \mathbb{R}^s$ ).

Further, a detailed scalar set of component databases is employed, which includes data related to key hydraulic components, such as cylinders, servovalves, accumulators, electric motors etc. The databases consist of records with real industrial data. Of those, for example, the electric motor database includes records with fields containing data such as motor nominal power, rpm, torque, voltage, current, weight and cost. Table 1 presents fields for hydraulic components records. In these records, additional data fields can be added as needed.

Any given load trajectory can be the input to the program and is supplied to the system integrated equations subroutine. An initial design parameter vector,  $\mathbf{d}_0$ , is selected to start the optimization procedure. Then, the integrated system equations subroutine computes the required actuator forces / torques and variables such as pressures, power, etc. Some of these variables, for example pressures, flows, power, areas, etc., are used to enter a specific database, which returns associated component values, such as buckling limits, allowable diameter ratios, weights and costs, needed in evaluating the problem constraints and calculating objective functions.

Depending on whether the constraints are satisfied or not, an appropriate update of the design vector  $\mathbf{d}$  is computed and the iterations continue till a minimum is reached for the objective function.

When the optimum solution  $\mathbf{d}^*$  is obtained, all other component parameters become available from the component database. A simplified flow chart of the optimization procedure is depicted in Fig. 2.

**Table 1:** Records of electrohydraulic component databases, including typical fields

Component record	field 1	field 2	field 3	field 4	field 5	field 6	field 7	field 8
Electric motor	power	torque	rotat. speed	voltage	current		weight	cost
Pump	volumetric displacement		rotational speed	power		maximum pressure	weight	cost
Cylinder	piston diameter	rod diameter	diameter ratio	stroke	buckling limit	maximum pressure	weight	cost
Hydraulic motor	volumetric displacement		rotational speed	power		maximum pressure	weight	cost
Accumulator	volume		pressure	charge pressure		max. pressure	weight	cost
Servovalve	nominal flow		nom. pressure	min. valve resistance		max. pressure	weight	cost

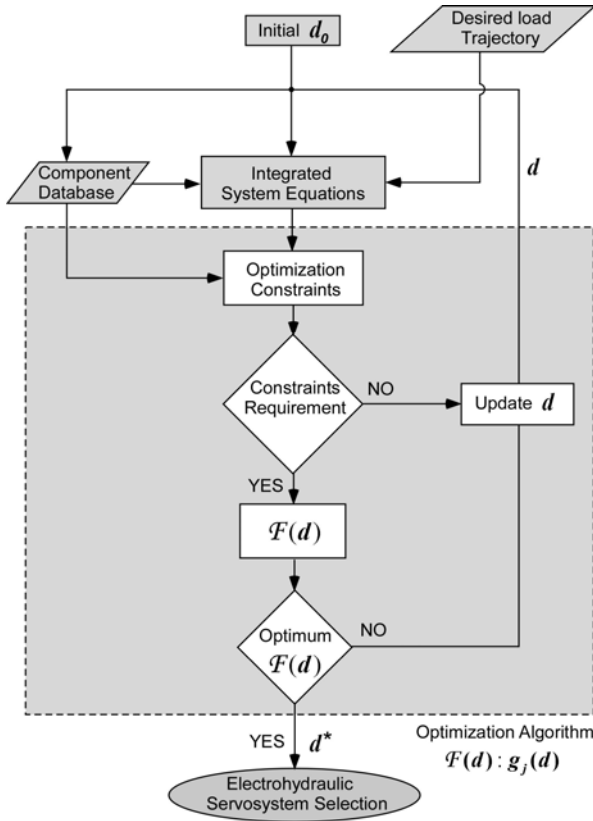


Fig. 2: Simplified optimization procedure flow chart

A number of optimization methods exist (Luenberger, 1989), that solve such problems. Of those, the most acknowledged and easy to use are the Newton - Raphson algorithms and the Sequential Quadratic Programming (SQP). The SQP method is a generalization of Newton's method for unconstrained optimization, in which a quadratic sub - problem is solved at each major iteration. This method is preferred because it is considerably faster than Newton - Raphson based algorithms, it enjoys the speed of the Sequential Linear Programming (SLP) algorithms and retains the good convergence properties of the Newton - Raphson algorithm. SLP algorithms are based on linearization of the Karush Kuhn Tucker (KKT) equations for the original nonlinear problem (Luenberger, 1989). Based on the above observations, the SQP method was employed here.

To use the SQP method, first a Lagrangian function of the optimization problem is defined as

$$L(d, \lambda) = F(d) + \sum_{j=1}^n \lambda_j \cdot g_j(d) \quad (18)$$

where  $\lambda_j$  are Lagrange multipliers. The SQP method replaces the constraint functions by linear approximations and the objective function with its quadratic approximation  $Q_k$ ,

$$Q_k(h) = \nabla F(d_k)^T h + \frac{1}{2} h^T H_k h \quad (19)$$

where  $h \in \mathbb{R}^n$  is the new vector of design parameters, pointing along the direction from the current point solution to the unconstrained optimum point of the problem. The matrix  $H_k$  is defined as the positive definite approximation of the Hessian matrix of the Lagrangian function, given by Eq. 18.

For the formulation given by Eq. 17, the vector  $h$  at step  $k$ ,  $h_k$ , is calculated by solving the quadratic subprogram

$$\min_{h \in \mathbb{R}^n} \left\{ \begin{aligned} Q_k(h) : \nabla g_j(d_k)^T h + g_j(d_k) \leq 0, \quad j \in I_1 \\ \nabla g_j(d_k)^T h + g_j(d_k) = 0, \quad j \in I_2 \end{aligned} \right\} \quad (20)$$

This subproblem can be solved using a Quadratic Programming algorithm. If  $h_k = 0$ , the current point is optimal with respect to the working set. If  $h_k \neq 0$  and  $d_k + h_k$  is feasible for all constraints, then  $d_k + h_k$  becomes the new  $d_{k+1}$ . If  $d_k + h_k$  is not feasible, the solution is used to form a new iterate with

$$d_{k+1} = d_k + a_k h_k \quad (21)$$

where the step length parameter,  $a_k$ , is determined by an appropriate line search procedure, so that a sufficient decrease in the objective function is obtained (Luenberger, 1989). Although the SQP method does not guarantee an absolute minimum, a reasonable selection of the initial  $d_0$  is usually sufficient for obtaining an optimum solution.

The optimization code is built in Matlab (The Language of Technical Computing, Ver. 6) and the minimization algorithm is provided by the Matlab Optimization Toolbox. The next section describes an application example in which the optimization methodology is presented in some detail.

## 4 Single DOF Electrohydraulic Servomechanism

In this section, the proposed methodology for the optimal component selection of a hydraulic servosystem is applied to the design of one-degree-of-freedom electrohydraulic servomechanism. This servo is to be used as an actuator in a robotic Stewart type mechanism, i.e. a six dof (degree-of-freedom) closed kinematic chain mechanism consisting of a fixed base and a movable platform with six linear actuators supporting it. The one dof mechanism is illustrated schematically in Fig. 3. The dynamic model for this system is presented next.

The angles of inclination of the actuator  $\theta$  and the load  $\varphi$  shown in Fig. 3 can be expressed as function of

the displacement of the actuator,  $x_p$ . Applying the Lagrange formulation, the equation of motion is written as

$$M(x_p) \ddot{x}_p + V(x_p, \dot{x}_p) + G(x_p) = F_p \quad (22)$$

where  $M(x_p)$  is a positive definite function, which represents the variable apparent mass of the mechanism, as seen by the actuator,  $V(x_p, \dot{x}_p)$  contains the Coriolis and centrifugal terms,  $G(x_p)$  represents the gravity term and  $F_p$  is the force applied to the mechanical load. The apparent mass  $M(x_p)$  the gravity term  $G(x_p)$  and the Coriolis and centrifugal terms  $V(x_p, \dot{x}_p)$ , are given in Appendix A.

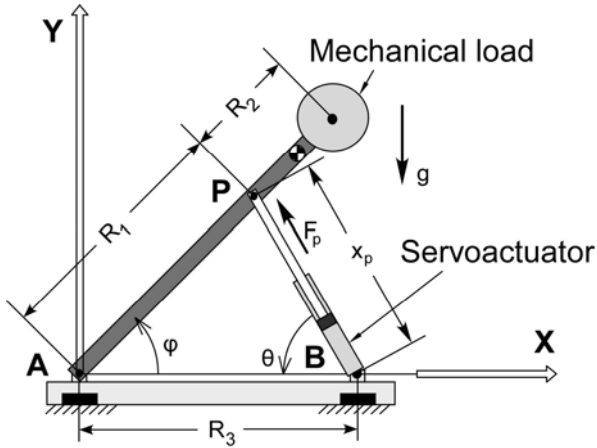


**Fig. 3:** Schematic view of the one DOF servomechanism model

The hydraulics equations of the servomechanism are described by Eq. 3-12 of Section 2. One of the most important characteristics is the  $Q_v - \Delta p_v$  servovalve curve, described in Section 2. Since the flow at the orifice is turbulent, this curve is described by a square root law, given by Eq. 4. The flow through the cylinder and the piston output force applied to the load are given by Eq. 3a-b and 3c correspondingly. The pressure drop at the servovalve is expressed by Eq. 9, neglecting line and auxiliary elements pressure drops. Finally, the hydraulic pump power is estimated by Eq. 8. The integrated system equations are given in Appendix A.

To select hydraulic components optimally, an objective function must be minimized, Eq. 15. The design parameters include the constant pressure of the power unit,  $d_1 = p_s$ , the rod diameter of the actuator,  $d_2 = b$ , the ratio  $d_3 = \mu = b/B$  of the rod diameter over the bore diameter,  $B$ , of the actuator and the minimum valve resistance coefficient  $d_4 = C_{R, \min, v_n}$ , where  $v_n$  is the valve number. All other systems parameters can be expressed as functions of these three, or depend on these through the database data. For example, the piston areas can be written as

$$A_1 = \pi d_2^2 d_3^{-2} / 4 \quad (23a)$$

$$A_2 = \pi d_2^2 (d_3^{-2} - 1) / 4 \quad (23b)$$

The combination of Eq. 3a, 3b and 23 provides the load flows through the two chamber ports of the hydraulic cylinder,

$$Q_{L,p1} = \pi d_2^2 d_3^{-2} \dot{x}_p / 4 \quad (24a)$$

$$Q_{L,p2} = \pi d_2^2 (d_3^{-2} - 1) \dot{x}_p / 4 \quad (24b)$$

The orifice areas of the cylinder chambers are considered symmetrical and the valve pressure drop at each valve orifice are expressed by

$$d_1 - p_{L,p1} = C_R Q_{L,p1} |Q_{L,p1}| \quad (25a)$$

$$p_{L,p2} = C_R Q_{L,p2} |Q_{L,p2}| \quad (25b)$$

The piston output force applied to the load, which is expressed by Eq. 3c is given by

$$F_p = [p_{L,p1} - p_{L,p2} (1 - d_3^2)] \pi d_2^2 d_3^{-2} / 4 \quad (26)$$

The combination of Eq. 24, 25 and 26 yields the pressures in the two chambers of the cylinder,

$$p_{L,p2} = (A_1 d_1 - F_p) A_2^2 / (A_2^3 + A_1^3) \quad (27a)$$

$$p_{L,p1} = (F_p + A_2 p_{L,p2}) A_1^{-1} \quad (27b)$$

where  $F_p$  is given by Eq. 22. Further, the evolution of the resistance coefficient  $C_R$  is calculated using Eq. 25.

Equation 22, 24, 25 and 27 consist of the integrated system equations, which are used in the optimization algorithm, see Fig. 2.

The power of the hydraulic supply is selected, as the objective function of interest. Similar results are obtained using the weight or cost objective functions. The pump power, given by the first equation of Eq. 15, is calculated combining Eq. 24a and 8, as

$$P = \pi d_1 d_2^2 d_3^{-2} \dot{x}_p / 4 \quad (28)$$

In order to bound the solution and to ensure a practical realization, the objective function is subject to constraints, that are imposed by material and fatigue strength (e.g. buckling critical diameters, etc.), design criteria, and technical and physical specifications. These constraints, are written as

$$-d_2 + b_{cr} \leq 0 \quad (29a)$$

$$d_2 - b_{max} \leq 0 \quad (29b)$$

$$-d_3 + \mu_{min} \leq 0 \quad (29c)$$

$$d_3 - \mu_{max} \leq 0 \quad (29d)$$

where  $b_{cr} = (64s_1s_2\ell_{cr}^2F_{p,max}/E\pi^3)^{0.25}$  is the buckling critical rod diameter of the piston,  $s_1$  is the buckling safety coefficient,  $s_2$  is the safety coefficient which is taking into account the relief valve extra pressure,  $\ell_{cr}$  is the buckling critical length of the piston,  $F_{p,max}$  is the maximum actuator force computed by the dynamic model analysis during the optimization,  $E$  is the modulus of elasticity,  $b_{max}$  is the maximum rod diameter of the piston, which is taken from the component database and  $\mu_{min}$ ,  $\mu_{max}$  are the minimum and the maximum values of the ratio  $\mu$  respectively, according to the component database.

During a cycle, the computed  $Q-\Delta p$  load curve should lie below the valve pressure – flow characteristic  $Q_v-\Delta p_v$ , otherwise a larger valve must be specified. Therefore, to drive the load successfully, a servovalve constraint is added to the optimization problem. This is given by

$$-d_4 + C_{R,min} \leq 0 \quad (30)$$

where  $C_{R,min}$  is the minimum valve resistance, over time  $t$ , given by

$$C_{R,min} = \min_t \left( \frac{\Delta p_v}{Q_v^2} \right) \quad (31)$$

In addition to the above constraints, physical constrains, due to the kinematics of the mechanism, may bound its variables. For example, static stability considerations and mechanism geometry require that

$$\varphi_{min} \leq \varphi(t) \leq \varphi_{max} \quad (32)$$

where  $\varphi_{min}$ ,  $\varphi_{max}$  are the minimum and maximum angle of load inclination, respectively.

Moreover, the optimization problem must satisfy an equality constraint due to pressure compatibility and given by

$$d_1 - \Delta p_v - |p_{L,p1} - p_{L,p2}| = 0 \quad (33)$$

where  $\Delta p_v$  is the servovalve pressure drop and is given by Eq. 10b.

In this example, one equality and six inequality constraints must be satisfied, i.e., the dimension of the system inequality constraints in Eq. 16a is  $p_1=7$  and the dimension of the system equality constraints in Eq. 16b is  $p_2=1$ .

## 5 Implementation Results

The mechanism parameters given include the load mass and inertia,  $m = 300$  kg and  $I = 1.6$  kgm<sup>2</sup>, the load supportive beam mass and inertia,  $m_1 = 10$  kg,  $I_1 = 4.8$  kgm<sup>2</sup> and geometrical parameters such as  $R_1 = 1.1$  m,  $R_2 = 1.1$  m and  $R_3 = 1.6$  m, see Fig. 3. The

initial design vector is taken as  $d_0 = [50 \text{ bar}, 0.01 \text{ m}, 0.4, 0.19 \text{ bar}/(\text{lpm})^2]^T$ .

The desirable trajectory of the load is given by

$$\varphi(t) = \varphi_s + \varphi_0 \cos \omega t \quad (34)$$

where  $\varphi_s = 70^\circ$  is the initial angle of inclination,  $\varphi_0 = 10^\circ$  is the amplitude of oscillation,  $\omega = 2\pi f$  is the angular velocity and  $f = 0.5$  Hz is the frequency of excitation. Of course, any other trajectory can be used equally well. The bounds of the load inclination angle are taken  $\varphi_{min} = 45^\circ$  and  $\varphi_{max} = 80^\circ$ .

**Case 1.** It is assumed initially that the system does not include an accumulator. Following the execution of the optimization procedure, the optimum design parameter vector  $d^* = [105.35 \text{ bar}, 0.027 \text{ m}, 0.65, 0.047 \text{ bar}/(\text{lpm})^2]^T$  is obtained. The corresponding objective function value is  $P = 6.05$  kW, after 27 iterations. Table 2 displays the basic ratings and sizes of the resulting servosystem. The pump power returned by the database is the next available pump rating, larger than 6.05 kW. Similarly, the motor rating corresponds to the next available rating for three phase induction motors. The total cost and weight, which corresponds to the optimum design vector can be easily computed using database information.

**Table 2:** Electrohydraulic element selection (Case 1)

Servomechanism			
Servocylinder		Servovalve	
Stroke	600 mm	Nominal pressure	
Bore diameter	0.04 m	drop 7 MPa	
Rod diameter	0.028 m	Nominal flow 38 lpm	
Weight	32.9 kg	Weight	1.1 kg
Power Supply Unit			
Hydraulic pump power	6.125 kW, (maximum displacement 23 cm <sup>3</sup> /rev)		
Hydraulic pump weight	20.4 kg		
Electric motor power	7.5 kW		
Electric motor weight	64 kg		

Figure 4 shows the plots of the resulting  $Q-\Delta p$  curve for the driven mechanical load along the desired trajectory. Also, three flow-pressure characteristics curves for three different servovalves are plotted at 100% open orifice. It is noticed that the valve with nominal flow 19 lpm is not adequate for the load requirements, while the nominal flow 63 lpm servovalve is oversized. The two load plots lie just under the characteristic of the servovalve with nominal flow 38 lpm and therefore, the procedure selects this servovalve as adequate for the designed servosystem.

The total execution time, when the optimization algorithm runs on a PIII / 800 MHz / RAM 128 MB PC, is about 3 min.

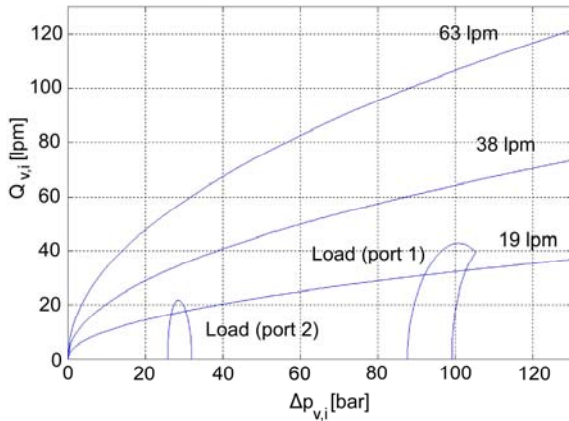


**Fig. 4:** Load and three fully orifice open servovalve  $Q_v-\Delta p_v$  curves

**Case 2.** Table 3 presents results when an accumulator is added to the power supply. As expected, here the hydraulic pump and electric motor ratings are lower than before. For instance, the total weight of the electric motor, the hydraulic pump and the accumulator is estimated to be 71.7 kg while in the first case it is computed to be 84.4 kg, i.e. a reduction of 17.7%.

**Table 3:** Electrohydraulic element selection (Case 2)

Hydraulic accumulator volume	1 L (bladder type)
Hydraulic accumulator weight	4.5 kg
Hydraulic pump power	4.26 kW, (maximum displacement 16 cm <sup>3</sup> /rev)
Hydraulic pump weight	13.2 kg
Electric motor power	5.5 kW
Electric motor weight	54 kg

Figure 5 illustrates the time varying flow of the hydraulic pump during one duty cycle of the servomechanism (forward and return flow direction) when no accumulator is present. In the presence of the accumulator, the flow is smoothed out at 20.47 lpm. Then, the cross section area 2 of the diagram is equal to the cross section area 1. Areas 1 and 2 represent the charge and discharge flow to the accumulator. Figure 6 illustrates the selected electrohydraulic components as part of the implemented hydraulic circuit.

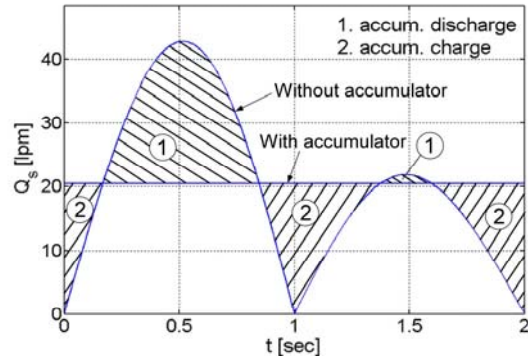


**Fig. 5:** Diagram of the time varying flow and the accumulator contribution

The results of the optimization presented in case 2 were used to build a servomechanism shown in Fig. 7a. This includes a custom made MOOG cylinder, a MOOG G761-Series servovalve and an MTS R-Series magnetostrictive position sensor. This servomechanism corresponds to a single leg of a high performance Stewart-type simulator (Stewart, 1965-66), currently in the design phase at NTUA.

The hydraulic power supply, shown in Fig. 7b, is equipped with a PARKER PVP41-Series piston pump, an SB 330 Series accumulator and a VALIADIS K-Type 3-phase electric motor.

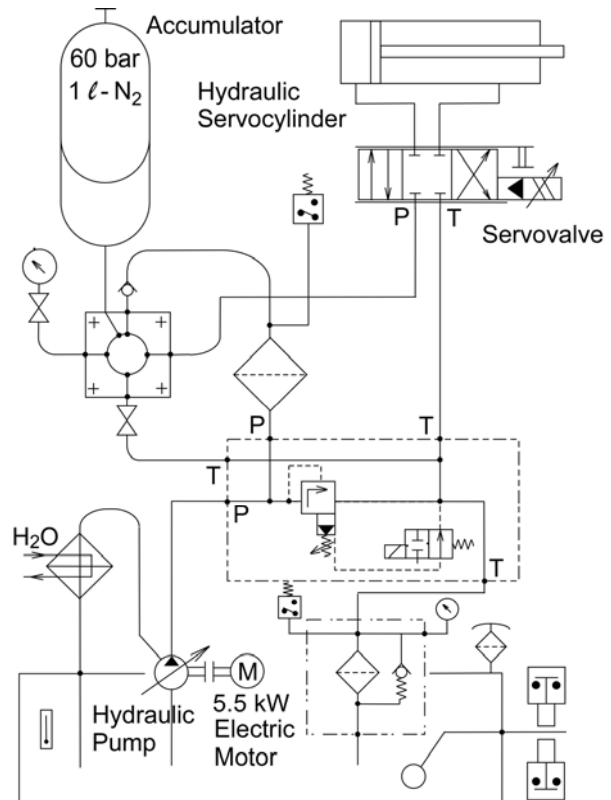


**Fig. 6:** The implements hydraulic circuit, highlighting selected components



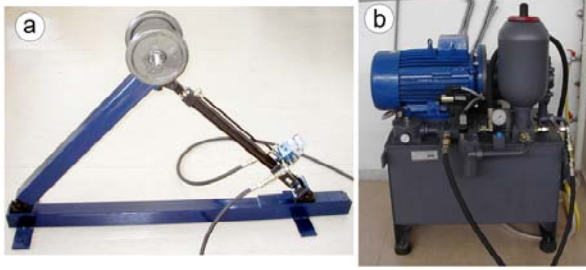


**Fig. 7:** The final setup; a. The driven load and its servomechanism, b. The hydraulic power supply

## 6 Conclusions

This paper focused on the optimal electrohydraulic component selection for servohydraulic robotic tasks. The proposed methodology required as its input a set of desired trajectories of the controlled mechanism and a description of the mechanism itself. Outputs included the complete specification of the system components such as the electric motor, the hydraulic pump, the hydraulic accumulator, the servovalve and the hydraulic servoactuator. Dynamic models for the electrohydraulic actuation system and its mechanical load (mechanism) were used to compute the optimal design parameters that minimize an objective function that may include the hydraulic supply power rating, the total weight, or the total cost. To this end, the Sequential Quadratic Programming (SQP) was employed as the optimization algorithm. The optimization procedure used component databases with real industrial data, resulting in realizable designs. The paper presented a detailed example in which the proposed methodology was applied.

## Nomenclature

$A$	piston area	$[m^2]$
$b$	rod diameter	$[m]$
$B$	bore diameter	$[m]$
$C$	cost	$[\$]$
$C_f$	fluid capacitance	$[m^4s^2/kg]$
$C_R$	resistance coefficient	$[kg/m^7]$
$C_{R,min}$	min. valve resistance coefficient	$[kg/m^7]$
$C_{im}$	internal leakage coefficient	$[m^4s/kg]$
$C_{em}$	external leakage coefficient	$[m^4s/kg]$
$d$	design parameter	
$\mathbf{d}$	design parameters vector	
$\mathbf{d}_0$	initial design parameter vector	
$\mathbf{d}^*$	optimum design parameter vector	
$D_m$	hydraulic motor constant	$[m^3/rad]$
$E$	elasticity modulus	$[N/m^2]$
$F_p$	piston force	$[N]$
$F$	objective function	

$g$	gravity acceleration	$[m/s^2]$
$\mathbf{g}$	constraint vector	
$G$	gravity term	$[N]$
$\mathbf{G}$	gravity vector	
$\mathbf{h}$	design parameters vector	
$\mathbf{H}$	hessian matrix	
$I$	moment of inertia	$[kgm^2]$
$K_t$	total kinetic energy	$[J]$
$l$	length	$[m]$
$\mathbf{L}, L$	lagrangian	
$m$	mass	$[kg]$
$M$	apparent mass	$[kg]$
$\mathbf{M}$	mass matrix	
$P$	power	$[W]$
$p$	pressure	$[N/m^2]$
$\Delta p$	pressure drop	$[N/m^2]$
$Q$	flow rate	$[m^3/s]$
$Q^*$	maximum flow	$[m^3/s]$
$Q_k$	quadratic approximation	$[m^3/s]$
$\mathbf{q}$	generalized coordinates vector	
$R$	length	$[m]$
$S$	orifice area	$[m^2]$
$s$	safety coefficient	$[-]$
$t$	time	$[s]$
$T$	torque	$[Nm]$
$v$	linear velocity	$[m/s]$
$V$	centrifugal and Coriolis term	$[N]$
$\mathbf{V}$	centrifugal and Coriolis vector	
$V_t$	total potential energy	$[J]$
$\mathbf{u}$	input vector	
$W$	weight	$[kg]$
$\mathbf{x}$	state vector	
$x$	linear displacement	$[m]$
$\mathbf{y}$	output vector	
$\theta$	angle	$[rad]$
$A$	sum of mass · length products	$[mkg]$
$\lambda_j$	Lagrange multipliers	
$\mu$	diameters ratio	$[-]$
$\rho$	fluid density	$[kg/m^3]$
$\boldsymbol{\tau}$	torque / force vector	
$\varphi$	angle	$[rad]$

## Indices

c	accumulator
cr	critical
cyl	cylinder
em	external
eq	equivalent

f	fluid
im	internal (for leakage coefficients)
in	internal (for resistances)
k	integration step
L	load
m	motor
m1	hydraulic motor chamber 1
m2	hydraulic motor chamber 2
max	maximum
min	minimum
nom	nominal
p	piston
p1	piston chamber 1
p2	piston chamber 2
R	resistance
s	supply
t	total
v	valve
v <sub>n</sub>	valve number
v1	valve chamber 1
v2	valve chamber 2

## Acknowledgment

The authors wish to thank the anonymous reviewers for their constructive comments and suggestions. Support of this work by the Hellenic General Secretariat for Research and Technology (EPAN M. 4.3.6.1) and the NTUA (Protagoras 10) is acknowledged.

## References

- Biggs, M. C.** 1975. Constrained Minimization Using Recursive Quadratic Programming. *Towards Global Optimization* (L. C. W. Dixon and G. P. Szergo, eds.), North-Holland, pp. 341-349.
- Blackburn, J. F., Reethof, G. and Shearer, J. L.,** 1960. *Fluid Power Control*. Cambridge, MA: MIT Press.
- Bowling, A. and Khatib, O.** 2002. Actuator Selection for Desired Dynamic Performance. *Proc. of the 2002 IEEE/RSJ Int. Conf. On Intelligent Robots and Systems EPFL*, pp. 1966 – 1973.
- Chatzakos, P. and Papadopoulos, E.** 2003. On Model-Based Control of Hydraulic Actuators. *Proc. of RAAD '03, 12th International Workshop on Robotics in Alpe-Adria-Danube Region*, Cassino, Italy.
- Chatzakos, P.** 2002. Design, Modeling and Control of a High-Performance Electrohydraulic Servo-system. *Master Thesis*, in Greek, NTUA.
- Han, S. P.** 1977. A Globally Convergence Method for Nonlinear Programming. *Journal of Optimization Theory and Application*, Vol. 22, p. 297.
- Hansen, M. R. and Andersen, T. O.** 2001. A Design Procedure for Actuator Control Systems Using Optimization Methods. *The 7th Scandinavian International Conference on Fluid Power*, Linköping, Sweden.
- Hansen, M. R., Andersen, T. O. and Conrad, F.** 2001. Experimentally Based Analysis and Synthesis of Hydraulically Actuated Loader Crane. *Power Transmission and Motion Control (PTMC 2001)*, Bath, UK.
- Herman, T., Bonicelli, B., Sevila, F., Monsion, M. and Bergeon, B.** 1992. Bond-graph modeling and identification of a high power hydraulic system. *In Proc. 11th IASTED Int. Conf. Modelling, Identification and Control*, Innsbruck, Austria.
- Jelali, M. and Kroll, A.** 2003. *Hydraulic Servo-systems. Modelling, Identification and Control*. Springer.
- Krus, P., Jansson, A. and Palmberg, J-O.** 1991. Optimization for Component Selection in Hydraulic Systems. *4th Bath International Fluid Power Workshop*, Bath, UK.
- Luenberger, D. G.** 1989. *Linear and Nonlinear Programming*, Second Edition.
- Matlab** 2000. *The Language of Technical Computing*, The Math Works Inc.
- Merritt, H. E.** 1967. *Hydraulic Control Systems*. J. Wiley.
- Papadopoulos, E. and Sarkar, S.** 1997. The Dynamics of an Articulated Forestry Machine and its Applications. *Proc. IEEE Int. Conference on Robotics and Automation*, pp. 323 – 328.
- Papadopoulos, E. and Gonthier, Y.** 2002. On the Development of a Real-Time Simulator Engine for a Hydraulic Forestry Machine. *Int. Journal of Fluid Power* 3, No. 1, pp. 55-65.
- Papadopoulos, E., Mu, B. and Frenette R.** 2003. On Modeling, Identification, and Control of a Heavy-Duty Electrohydraulic Harvester Manipulator. *IEEE/ASME Transactions on Mechatronics*, Vol. 8, No. 2, pp. 178 - 187.
- Rosenberg, R. and Karnopp, D.** 1983. *Introduction to Physical System Dynamics*. McGraw Hill, New York, NY.
- Rowell, D. and Wormley, D.** 1997. *System Dynamics*. Prentice Hall.

**Six, K. and Lasky, T. A.** 2001. A Time-Delayed Dynamic Inversion Scheme for Mechatronic Control of Hydraulic Systems. *IEEE/ASME Int. Mechatronics Proc.*, pp. 1232 – 1238.

**Stewart, D.** 1965-66. A platform with six degrees of freedom. *Proceedings of the IMechE*, Vol. 180, Pt. 1, No 15, pp. 371-385.

**Thayer, W. J.** 1962. Specification Standards for Electrohydraulic Flow Control Servovalves. *Techn. Bull.* 117, Moog Inc. Control Div., E. Aurora, NY.

**Van de Straete, H. J., Degezelle, P. and De Schutter, J.** 1998. Servo Motor Selection Criterion for Mechatronic Application. *IEEE/ASME Transactions on Mechatronics*, Vol. 3, No 1, pp. 43 – 50.

## Appendix A

### Mechanical Load Dynamics

The equation of motion for the mechanical load is derived applying the Lagrange formulation given by Eq. 22. To this end, the Lagrangian is given by

$$L = K_t - V_t \quad (A1)$$

where  $K_t$  and  $V_t$  are the total kinetic and potential energy of the servosystem respectively, which are given by

$$K_t = [I_{eq,L} \dot{\varphi}^2 + m_{eq,cyl} \dot{x}_p^2 + I_{eq,cyl} \dot{\theta}^2] / 2 \quad (A2a)$$

$$V_t = [(R_1 + R_2) m_{eq,L} \sin \varphi + (x_p m_{eq,p} + A_{eq,cyl}) \sin \theta] g \quad (A2b)$$

where  $x_p$  is the displacement of the actuator,  $g$  is the acceleration of gravity,  $\varphi$ ,  $\theta$ ,  $R_1$  and  $R_2$  are defined in Fig. 3,  $I_{eq,L}$  is the equivalent load moment of inertia, which includes the load and the load supportive beam mass moments of inertia, about their centers of mass,  $I_{eq,cyl}$  is the equivalent cylinder moment of inertia, which contains the cylinder, piston and oil moments of inertia, about their centers of mass,  $m_{eq,cyl}$  is the equivalent cylinder mass, which includes the piston and oil masses,  $m_{eq,L}$  is the equivalent load mass, which includes the load mass and the load mass of the supportive beam mass,  $m_{eq,p}$  is the equivalent piston mass, which comprises the piston rod and piston head masses and  $A_{eq,cyl}$  is the sum of the products of the cylinder masses times cylinder lengths, which includes the cylinder, piston and oil masses and cylinder and piston lengths.

In Eq. 22, the apparent mass  $M(x_p)$  the gravity term  $G(x_p)$  and the Coriolis and centrifugal terms  $V(x_p, \dot{x}_p)$  are given by

$$M(x_p) = m_{eq,cyl} + x_p^2 I_{eq,L} (R_1 R_2)^{-2} \csc^2 \varphi + (x_p \csc \theta - R_3 \cot \theta)^2 (x_p R_3)^{-2} I_{eq,cyl} \quad (A3a)$$

$$G(x_p) = g [x_p (R_1 + R_2) (R_1 R_2)^{-1} m_{eq,L} \cot \varphi + m_{eq,p} \sin \theta - (x_p - R_3 \cos \theta) \cdot (x_p R_3)^{-1} (x_p m_{eq,p} + A_{eq,cyl}) \cot \theta] \quad (A3b)$$

$$V(x_p, v_p) = \{ (x_p m_{eq,p} + A_{eq,p}) (x_p - R_3 \cos \theta)^2 (x_p R_3)^{-2} \csc^2 \theta - x_p I_{eq,L} \csc^4 \varphi \cdot (x_p^2 \cos \varphi - R_1 R_3 \sin^2 \varphi) (R_1 R_3)^{-2} + I_{eq,cyl} (x_p R_3)^{-3} \{ [(x_p - R_3 \cos \theta) \cdot \csc^2 \theta (x_p R_3 - R_3^2 \cos \theta - x_p R_3 \cdot \cot^2 \theta + x_p^2 \cot \theta \csc \theta) - R_3 \csc \theta \cdot (x_p \csc \theta - R_3 \cot \theta) (2x_p - 2R_3 \cdot \cos \theta + x_p \cot^2 \theta - R_3 \cot \theta \csc \theta)] \} \} v_p^2 \quad (A3c)$$

where  $R_3$  is defined in Fig. 3 and  $A_{eq,p}$  is the sum of the products of the piston masses times piston lengths, which includes the piston rod and piston head masses and piston rod and piston head lengths.



**Evangelos Papadopoulos**

Received his Diploma from the NTUA in 1981 and his M.S. and Ph.D. from MIT in 1983 and 1991 respectively, all in Mechanical Engineering (ME). He then joined the ME Dept. at McGill U. and he became an Assoc. Prof. in 1997. Currently, he is an Assoc. Prof. with the ME Dept. of NTUA. His research interests are in robotics, mechatronics, modelling and control of dynamic systems and electrohydraulic servo systems. He is a senior member of IEEE and AIAA and a member of ASME and Sigma Xi.



**Ioannis Davliakos**

Received his Diploma from the Aristotle University of Thessaloniki (AUTH), in 1998, in Mechanical Engineering. In 1999, he received the M.S. degree from the National Technical University of Athens (NTUA), where he is currently working towards a Ph.D. degree in Mechanical Engineering. His research interests are in electrohydraulic servo-systems, robotic parallel mechanisms and control of dynamic systems.